Long non-coding RNA MEG3 suppresses epithelial-to-mesenchymal transition by inhibiting the PSAT1-dependent GSK-3β/Snail signaling pathway in esophageal squamous cell carcinoma

MING-KAI LI[1*], LI-XUAN LIU[1*], WEI-YI ZHANG[1], HAO-LIAN ZHAN[1],
RUI-PEI CHEN[1], JIA-LIN FENG[2] and LING-FEI WU[1]

Departments of [1]Gastroenterology and [2]Information, Second Affiliated Hospital,
Shantou University Medical College, Shantou, Guangdong 515041, P.R. China

Abstract. Esophageal squamous cell carcinoma (ESCC) is the main subtype of esophageal cancer in China, and the prognosis of patients remains poor mainly due to the occurrence of lymph node and distant metastasis. The long non-coding RNA (lncRNA) maternally expressed gene 3 (MEG3) has been shown to have tumor-suppressive properties and to play an important role in epithelial-to-mesenchymal transition (EMT) in some solid tumors. However, whether MEG3 is involved in EMT in ESCC remains unclear. In the present study, the MEG3 expression level and its association with tumorigenesis were determined in 43 tumor tissues of patients with ESCC and in ESCC cells using reverse transcription-quantitative PCR analysis. Gene microarray analysis was performed to detect differentially expressed genes (DEGs). Based on the functional annotation results, the effects of ectopic expression of MEG3 on cell growth, migration, invasion and EMT were assessed. MEG3 expression level was found to be markedly lower in tumor tissues and cells. Statistical analysis revealed that MEG3 expression was significantly negatively associated with lymph node metastasis and TNM stage in ESCC. Fluorescence *in situ* hybridization assay demonstrated that MEG3 was expressed mainly in the nucleus. Ectopic expression of MEG3 inhibited cell proliferation, migration, invasion and cell cycle progression in EC109 cells. Gene microarray results

demonstrated that 177 genes were differentially expressed ≥2.0 fold in MEG3-overexpressing cells, including 23 upregulated and 154 downregulated genes. Functional annotation revealed that the DEGs were mainly involved in amino acid biosynthetic process, mitogen-activated protein kinase signaling, and serine and glycine metabolism. Further experiments indicated that the ectopic expression of MEG3 significantly suppressed cell proliferation, migration, invasion and EMT by downregulating phosphoserine aminotransferase 1 (PSAT1). In pathological tissues, PSAT1 and MEG3 were significantly negatively correlated, and high expression of PSAT1 predicted poor survival. Taken together, these results suggest that MEG3 may be a useful prognostic biomarker and may suppress EMT by inhibiting the PSAT1-dependent glycogen synthase kinase-3β/Snail signaling pathway in ESCC.

Introduction

Esophageal cancer (EC) is a particularly aggressive malignancy with a high mortality rate, which is the ninth most commonly diagnosed type of cancer and the sixth leading cause of cancer-related mortality worldwide (1). There are two types of EC, namely esophageal squamous cell carcinoma (ESCC) and esophageal adenocarcinoma. In China and other East Asian countries, up to 90% of cases are ESCCs (2). Shantou, in particular, is a high-risk area for ESCC. Due to the lack of early signs or symptoms in ESCC, endoscopic screening in the asymptomatic population is inadequate, and early diagnosis of ESCC is difficult. In the majority of the cases, at the time of endoscopy, the disease has already progressed to an advanced stage. Despite numerous advances over the last several decades, the prognosis of this disease remains poor, with a 5-year survival rate of <40% (3,4). Thus, it is urgent to explore the key protein-signaling networks and relative molecular regulatory mechanisms of ESCC.

Previous evidence indicates that the process of epithelial-to-mesenchymal transition (EMT) is a cellular switch from epithelial to mesenchymal cell properties, which promotes cancer progression (5,6). EMT often occurs at the

Correspondence to: Professor Ling-Fei Wu, Department of Gastroenterology, Second Affiliated Hospital, Shantou University Medical College, 69 Dongxia Road, Shantou, Guangdong 515041, P.R. China
E-mail: 1808435253@qq.com

early stages of tumor metastasis, and involves a disassembly of cell-cell junctions and enhancement of cell motility, accompanied by decreased expression of classic epithelial markers (E-cadherin and β-catenin) and increased expression of mesenchymal markers [N-cadherin, glycogen synthase kinase (GSK)-3β, vimentin and Snail] (7,8).

Recent studies have revealed that lncRNAs play key roles in the carcinogenesis and development of various types of cancer. The lncRNA maternally expressed gene 3 (MEG3) is widely expressed in a variety of normal tissues. MEG3 has been identified as a tumor suppressor and is expressed at lower levels in diverse types of cancer (9-13). However, whether MEG3 is involved in the EMT process of ESCC remains elusive.

The aim of the present study was to determine the expression levels of MEG3 in ESCC tissues and cells, and analyze its clinical significance. A recombinant lentiviral vector expressing MEG3 (Lv-MEG3) was constructed. Microarray technology and bioinformatics analysis were employed to study the differentially expressed genes (DEGs) between the two groups. Based on functional annotation results, the underlying target genes and the effects of ectopic expression of MEG3 on cell growth, migration, invasion and EMT were assessed *in vitro* and *in vivo*.

Materials and methods

Patients and human esophageal tissue specimens. A total of 43 cases of ESCC, which had been clinically and histologically diagnosed between 2011 and 2016, were included in the present study. The cohort comprised 25 men and 18 women (median age, 57.41 years; range, 36-75 years). Lymph node metastasis was detected in 28 cases, and 19 patients were diagnosed with grade I or II ESCC. None of the patients underwent radiotherapy or chemotherapy prior to surgery. Tumor masses and adjacent normal tissues, which were located ≥5.0 cm distal to the tumor margins, were divided into two parts. One part was snap-frozen in liquid nitrogen for reverse transcription-quantitative PCR (RT-qPCR) assay, and the other part was fixed in formalin and embedded in paraffin for immunohistochemistry assay. Written informed consent was obtained from each patient and all the procedures were approved by the Second Affiliated Hospital Ethics Committee of Shantou University Medical College (Shantou, China).

Cell culture. ESCC cell lines (EC109, EC-9706 and KYSE-450) and the normal esophageal epithelial cell line Het-1A were obtained from the Institute of Biochemistry and Cell Biology of the Chinese Academy of Sciences. Cells were cultured in DMEM supplemented with 10% (v/v) FBS (Invitrogen; Thermo Fisher Scientific, Inc.), 100 U/ml penicillin and 100 mg/ml streptomycin at 37°C in 5% CO_2.

Plasmid constructs and lentivirus-mediated MEG3 overexpression in ESCC cells. To construct the MEG3 overexpression lentiviral vector, the full-length coding sequence of the MEG3 gene (GenBank ID: NR_002766) was amplified by PCR and then cloned into the *Bam*HI/*Eco*RI sites of the pLenti-EF1a-EGFP-F2A-Puro-CMV-MEG3 vector (Obio Technology) using the following primers: Forward,

5'-CGCAAATGGGCGGTAGGCGTG-3' and reverse, 5'-CAT AGCGTAAAAGGAGCAACA-3'. The recombinant eukaryotic expression vector was constructed and confirmed by DNA sequencing, enzymatic digestion and PCR identification. For the production of viral particles, the lentivirus-mediated MEG3 packaging system containing MEG3 was co-transfected with packaging vectors (pLP1 and pLP2) and envelope vector (pLP/VSVG) into 293T cells with OGTR20131002 Transfection Reagent (Obio Technology) according to the manufacturer's instructions. After the recombinant lentiviral vector expressing MEG3 (Lv-MEG3) and the negative control (NC) empty vector (Lv-NC) were constructed, packaging, purification and titer determination were conducted in 293T cells, as described in our previous study (14).

Microarray analysis. EC109 cells were transfected with Lv-MEG3 or Lv-NC. Total RNA was extracted from Lv-MEG3 or Lv-NC cells using TRIzol® RNA isolation reagent (Invitrogen; Thermo Fisher Scientific, Inc.) according to the manufacturer's protocol. The gene expression profiles were performed based on the Affymetrix PrimeView™ Human Gene Expression Array (Affymetrix; Thermo Fisher Scientific, Inc.). Gene expression analysis was performed using GeneSpring software (version 14.8; Agilent Technologies, Inc.), and the data were shown by volcano plots. Cluster, Gene Ontology (GO) enrichment and Kyoto Encyclopedia of Genes and Genomes (KEGG) analyses were conducted using online tools (http://www.shbio.com/customer.php) to determine the DEGs. P-value and false discovery rate (FDR) were used to define the threshold of significance, and the figures were generated by R language. DEGs were identified by paired test [fold-change (FC) ≥2.0 or ≤0.5, P<0.05 and FDR<0.05]. The microarray data were uploaded in the National Center for Biotechnology Information Gene Expression Omnibus (GEO) database; GEO accession no., GSE142036 (https://www.ncbi. nlm.nih.Gov/geo/query/acc.cgi?acc=GSE142036).

Construction of a protein-protein interaction (PPI) network. The Search Tool for the Retrieval of Interacting Genes/Proteins (STRING; version 10.0; http://string-db.org) was employed to identify the interaction pairs of the overlapped target genes. The predicted and acknowledged interactions were unified and scored. Genes with a connectivity degree of ≥5.0 were considered as hub genes. Interaction pairs in the PPI network were selected when the combined score was >0.4.

Fluorescence in situ hybridization (FISH) and subcellular fractionation analysis. EC109 cells were transfected with Lv-MEG3 or Lv-NC, and immunofluorescence assays were performed as described previously (15). Digoxigenin-labeled MEG3 and FISH Kit (Exon Lab) were used following the manufacturer's instructions. MEG3 was visualized using HRP anti-digoxigenin-antibody (1:50; cat. no. ab6212; Abcam) at room temperature for 1 h, and tyramide signal amplification-FITC technology was used. EC109 cells were co-stained with DAPI and finally observed under a fluorescence microscope at a magnification of x1,000 (Nikon80i; Nikon Corporation). RNA was isolated as nuclear and cytoplasmic fractions in EC109 cells using the RNA Subcellular Isolation Kit (Norgen Biotek Corp.) according to the manufacturer's

guidelines. Cytoplasmic and nuclear fractions were analyzed by RT-qPCR.

Cell proliferation assay. Cell proliferation was analyzed with the Cell Counting Kit-8 (CCK-8) assay (Beyotime Institute of Biotechnology) according to the manufacturer's protocol. A total of 4,000 cells were seeded in triplicate in 96-well plates and transfected with Lv-MEG3 or Lv-NC plasmids for the indicated times. Cell viability was assessed by measuring the absorbance at 450 nm using the FilterMax F5 microplate reader (Molecular Devices, LLC).

Cell cycle analysis. After transfection for 48 h, EC109 cells ($1x10^5$ cells/ml) were harvested, washed with ice-cold PBS and fixed with 70% ethanol at 4°C overnight. After fixation, the cells were washed, resuspended in PBS, incubated with ribonuclease at 37°C for 30 min and stained with propidium iodide (Nanjing KeyGen Biotech Co., Ltd.) in the dark at 4°C for 30 min. Then, the cell cycle distribution was analyzed with a flow cytometer (BD Biosciences).

RT-qPCR analysis. Total RNA was extracted from freshly frozen ESCC tissues or transfected cells according to the instructions of the TRIzol® kit (Invitrogen; Thermo Fisher Scientific, Inc.). Subsequently, RT-qPCR was performed with a Step-One Plus Real-Time PCR System (Applied Biosystems; Thermo Fisher Scientific, Inc.) using the SYBR Green PCR Master Mix (Promega Corporation). The thermal cycling conditions were as follows: 95°C for 10 min, 95°C for 15 sec, and 58°C for 30 sec for 40 cycles. GAPDH was employed as an endogenous control. All the primer sequences used in this study are listed in the Table I. The relative expression level of mRNAs was calculated by the $2^{-\Delta\Delta Cq}$ method as described in our previous study (16).

Cell invasion assay. After transfection for 48 h, EC109 cells were seeded in a 6-well plate for 48 h and resuspended in serum-free DMEM at a cell density of $3x10^5$ cells/ml. Then, 200 µl cell suspension was added to the apical chamber, while 500 µl DMEM containing 10% FBS was added to the basolateral chamber, and incubated at 37°C in the presence of 5% CO_2. After 24 h, the invading cells were fixed at 4°C with methanol for 10 min, washed with PBS 3 times and stained at room temperature with 0.1% crystal violet solution for 10 min. A neutral resin was applied to seal the cells in the apical chamber, and 6 randomly selected fields were observed with an inverted microscope (Axiovert 40 CFL, Carl Zeiss AG) microscope at a magnification of x100.

Wound healing assay. After transfection with Lv-MEG3 or Lv-NC for 48 h, EC109 cells ($1x10^6$ cells/ml) were added to a 6-well plate and incubated for 24 h. After the cells had reached 90-100% confluence, a sterile 1-ml pipette tip was used to create a linear scratch in the cell monolayer. After culturing with FBS-free medium at 37°C for different durations, the cells that migrated to the wounded area were visualized and images were captured with an Axiovert 40 CFL fluorescence microscope (Carl Zeiss AG) at 0, 24, 36 and 48 h. The rate of wound closure was measured using ImageJ software (version 1.46; National Institutes of Health).

Table I. Primer sequences for reverse transcription-quantitative PCR analysis.

Gene	Primer sequence (5'-3')
MEG3	Forward, TGGGTCGGCTGAAGAACTG
	Reverse, CCAAACCAGGAAGGAGACGA
PSAT1	Forward, CTCAGGCAGGATCTGGCATA
	Reverse, CCTGGAGTGCTGTTGGAGAA
VEGFA	Forward, CCTTCGCTTACTCTCACCTGCTTC
	Reverse, GGCTGCTTCTTCCAACAATGTGTC
U6	Forward, CTCGCTTCGGCAGCACATA
	Reverse, AACGATTCACGAATTTGCGT
GAPDH	Forward, CACCATCTTCCAGGAGCGA
	Reverse, TCAGCAGAGGGGGCAGAGA

MEG3, maternally expressed gene 3; PSAT1, phosphoserine amino-transferase 1; VEGFA, vascular endothelial growth factor A.

Protein extraction and western blotting. EC109 cells transfected with Lv-MEG3 or Lv-NC were harvested at 48 h and washed with ice-cold PBS 3 times. The cell lysates were prepared with RIPA buffer (Beyotime Institute of Biotechnology) containing PMSF. Equal quantities of proteins (50 µg) were separated by 10% SDS-PAGE and transferred to PVDF membranes. After being blocked with 5% non-fat milk for 60 min at room temperature, the membranes were incubated with specific primary antibodies against PSAT1 (1:1,000; cat. no. GTX82102; GeneTex, Inc.), cyclin D1 (CCND1; 1:1,000; cat. no. sc-8396; Santa Cruz Biotechnology, Inc.), phosphorylated (p)-GSK-3β (1:500; cat. no. ab75745; Abcam), GSK-3β (1:500; cat. no. ab32391; Abcam), E-cadherin (1:1,000; cat. no. sc-21791; Santa Cruz Biotechnology, Inc.), Snail (1:1,000; cat. no. sc-271977; Santa Cruz Biotechnology, Inc.), vascular endothelial growth factor (VEGF)A (1:1,000; cat. no. Ag13500; ProteinTech Group, Inc.), vimentin (1:5,000; cat. no. GTX100619; GeneTex, Inc.), β-actin (1:500; cat. no. ab8226; Abcam) or GAPDH (1:5,000; cat. no. sc-166574; Santa Cruz Biotechnology, Inc.) as an internal control in TBS-0.5% Tween-20 (TBST) at 4°C overnight. On the following day, the membranes were washed with TBST 3 times and incubated by anti-rabbit horseradish peroxidase-conjugated secondary antibody (1:10,000; cat. no. sc-2004; Santa Cruz Biotechnology, Inc.) at room temperature in the dark for 60 min. The expression of proteins was measured with the Odyssey Detection System (LI-COR Biosciences) and analyzed using ImageJ software, version 1.46r (National Institutes of Health).

In vivo tumorigenesis assay. The animal protocols in the present study were approved by the Ethics Committee of Shantou University Medical College. A total of 19 male BALB/c nude mice (class SPF, purchased from Beijing Animal Center), aged 6-weeks and weighing 18-24 g, were subcutaneously injected in the right flank with $8x10^6$ EC109 cells transfected with Lv-MEG3 (experimental group) or Lv-NC (control group) in 0.1 ml PBS. Tumor volume (V) was measured with calipers and calculated with the formula $V=0.52xLxW^2$ (where L and

W are the long and short axes of the tumor, respectively). After 3-4 weeks, the mice were anesthetized by inhalation of 5% isoflurane and sacrificed by cervical dislocation. Death was confirmed based cessation of convulsions and sustained absence of breathing. The tumors were excised and weighed. The target molecules in the tumor tissues were detected by western blotting.

Immunohistochemical analysis. Formalin-fixed tissues were embedded in paraffin and 4-μm sections were cut from each paraffin block. The paraffin sections were dewaxed in xylene twice for 15 min each and rehydrated through a graded series of alcohol solutions (5 min per step). The slides were then stained with the primary antibody (rabbit anti-PSAT1 antibody; dilution, 1:100; cat. no. sc-133929; Santa Cruz Biotechnology, Inc.) at 4˚C overnight. The sections were then washed in PBS and incubated at room temperature for 20 min with biotinylated secondary antibody, followed by incubation at room temperature for 10 min with streptavidin-peroxidase complex (Histostain-Plus Kit, Invitrogen; Thermo Fisher Scientific, Inc.). The chromogen 3,3'-diaminobenzidine was then added, and the sections were subsequently counterstained for 2 min at room temperature with Mayer's hematoxylin. Negative control sections were treated as described above, but the primary antibody was omitted. Two pathologists blinded to the clinical information independently assessed the immunohistochemistry results. In total, 5 visual fields were randomly selected in each section, and 200 tumor cells were counted in each visual field at x200 magnification. According to the percentage of positive cells marked by yellow particles observed in tissues, the PSAT1 staining index (SI) was scored according to staining intensity (0, negative; 1, weak, light yellow; 2, moderate, yellow brown; and 3, strong, brown) multiplied by a distribution score (1, <10%; 2, 10-50%; and 3, >50% cells stained). An SI score ≥3 was defined as a high expression level of PSAT1, while SI scores 0-2 were considered to reflect a low expression level of PSAT1.

Statistical analysis. Statistical analyses were performed using SPSS software (version 22.0; IBM Corp.). All experiments in the present study were repeated ≥3 times, and the data are presented as the mean ± SD. Differences in mean values between groups were assessed for statistical significance using the Student's t-test. Welch's ANOVA test and Games-Howell post hoc test were applied to compare MEG3 expression among different cell lines. Pearson's correlation coefficient analysis was applied to calculate the correlation between the expression of MEG3 and PSAT1 in ESCC tissues. Survival curves were plotted using the Kaplan-Meier method and were analyzed using the log-rank test. P<0.05 was considered to indicate statistically significant differences.

Results

MEG3 expression is downregulated in ESCC tissues/cells and is associated with poor prognosis. The levels of MEG3 were evaluated in 43 pairs of ESCC tissues and corresponding adjacent normal tissues. The results indicated that MEG3 was significantly downregulated in ESCC tissues compared with its expression in normal controls (Fig. 1A). The expression

level of MEG3 was significantly reduced in tumor tissues, as described in our previous study (17). In addition, the association between MEG3 expression and lymph node metastasis in ESCC was investigated. As shown in Fig. 1B, the expression of MEG3 was significantly decreased in ESCC patients with lymph node metastasis compared with that in ESCC patients without lymph node metastasis. Moreover, the expression level of MEG3 was significantly reduced in aggressive ESCC (TNM stage III-IV; Fig. 1C), suggesting that the downregulation of MEG3 is associated with the development of ESCC. Additionally, the level of MEG3 in ESCC cell lines (EC109, EC-9706 and KYSE-450) was significantly lower compared with that in Het-1A cells (Fig. 1D). Among the three ESCC cell lines evaluated, EC109 exhibited the lowest expression of MEG3; thus, this cell line was used for subsequent experiments. Taken together, these findings suggest that MEG3 may play a role as a tumor suppressor gene in the development of ESCC.

Lentivirus-mediated MEG3 stable expression in EC109 cells. To further explore the biological relevance of MEG3 in EC109 cells, the cultured EC109 cells were infected with either Lv-MEG3 or Lv-NC, and then puromycin was employed for selection and enrichment of lentivirus-infected cells (Fig. 2A). The mRNA expression of MEG3 was significantly increased in the Lv-MEG3 group compared with that in the Lv-NC group (Fig. 2B), indicating that Lv-MEG3 was transfected into cells successfully, and a high mRNA expression level of MEG3 was observed in EC109 cells. FISH assay revealed that MEG3 was mainly distributed in the nucleus, and a small portion was distributed in the cytoplasm (Fig. 2C). The results of MEG3 subcellular localization were further confirmed by cytoplasmic and nuclear RNA fractionation analysis in EC109 cells (Fig. 2D).

Ectopic expression of MEG3 suppresses proliferation, migration and invasion in EC109 cells. To further elucidate the role of MEG3 in ESCC cell proliferation and cell cycle progression, Lv-MEG3 was stably transfected into EC109 cells. The results of the CCK-8 assay indicated that the ectopic expression of MEG3 obviously inhibited the proliferation of EC109 cells at 48, 72 and 96 h (Fig. 3B). Consistently with these results, cell cycle analysis demonstrated that the ectopic expression of MEG3 increased the proportion of cells in the G1 phase and decreased the proportion of cells in the S phase of the cell cycle (P<0.05; Fig. 3A). Furthermore, western blotting confirmed that CCND1, a key regulator of G1-to-S phase progression, was significantly decreased in the Lv-MEG3 group (Fig. 3C), which suggested that the ectopic expression of MEG3 inhibited cell proliferation likely through induction of G1 arrest by inhibiting CCND1. Moreover, Transwell migration and wound healing assays revealed that the ectopic expression of MEG3 markedly inhibited cell invasion and migration (Fig. 3D and E). These findings demonstrated that MEG3 suppressed the proliferation and motility of EC109 cells.

Identification of DEGs after overexpression of MEG3. DEGs in EC109 cells were identified after MEG3 was overexpressed through transfection with Lv-MEG3. In total, 177 genes (23 upregulated and 154 downregulated) were found to be differentially expressed in a microarray conducted for 3 pairs
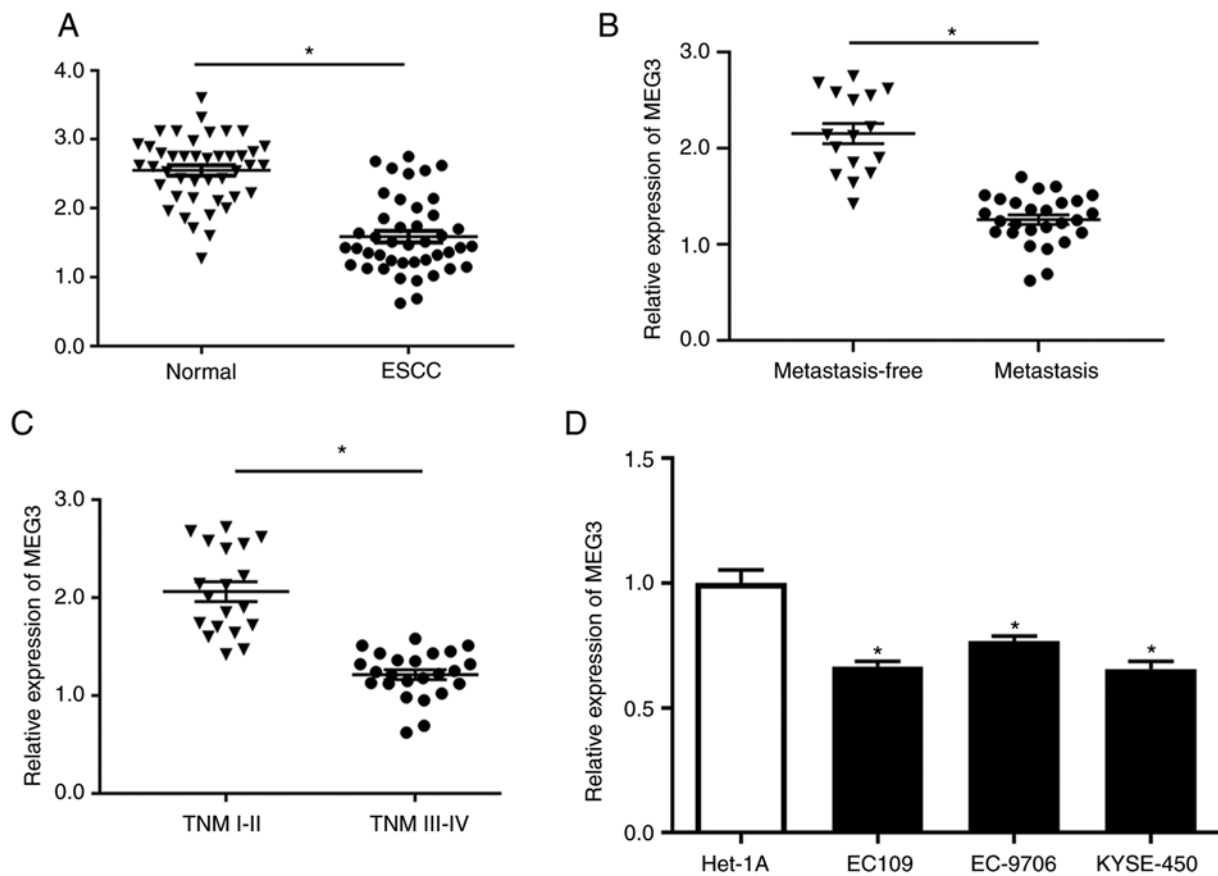
Figure 1. MEG3 is significantly downregulated in ESCC tissues/cells and is associated with poor prognosis. (A) The expression level of MEG3 was examined in 43 ESCC and adjacent normal tissues by reverse transcription-quantitative PCR analysis. (B) MEG3 expression was evaluated in patients with ESCC and lymph node metastasis (metastasis), and compared with that in ESCC patients without lymph node metastasis (metastasis-free). (C) MEG3 expression was evaluated in patients with TNM I-II and TNM III-IV stage ESCC. (D) The expression level of MEG3 was examined in the normal esophageal cell line Het-1A and in ESCC cells (EC109, EC-9706 and KYSE-450). *P<0.05. MEG3, maternally expressed gene 3; ESCC, esophageal squamous cell carcinoma.

of EC109 cells treated with Lv-MEG3 or Lv-NC (the threshold was set as FC >2.0 or <0.5). The 23 upregulated and the top 30 downregulated genes are listed in Table II. Scatter and volcano plots were used to assess gene expression variations between the Lv-MEG3 and Lv-NC groups (Fig. S1A and B). The relative expression levels of mRNAs among the matched samples were determined by hierarchical cluster analysis (Fig. S1C).

GO, KEGG pathway and PPI network analysis. Recent findings have identified numerous candidate oncogenes and tumor suppressor genes functioning in the one-carbon metabolism pathway. However, the expression levels of these molecules in ESCC remain unclear. To illustrate the functions of MEG3 in EC109 cells, Cytoscape 3.6 software was used to extract DEGs between the Lv-MEG3 and Lv-NC groups, and the STRING database was utilized to provide PPI information (18).

GO enrichment analysis demonstrated that these genes were significantly enriched in terms of serine family amino acid biosynthetic process, cellular response to glucose starvation and neutral amino acid transmembrane transporter activity (Fig. S2 and Table III). The most significant terms of the KEGG pathway included amino acid biosynthesis, aminoacyl-tRNA biosynthesis, serine and threonine metabolism, vitamin B6 metabolism, aspartate and glutamate metabolism and mitogen-activated protein kinase (MAPK) signaling pathway (Fig. S2; Table IV). The PPI network suggested that

PSAT1, PHGDH, ASNS, ASRS, MARS, ATF4 and VEGFA were significant genes, and they were considered as hub genes (Fig. S3).

Validation of DEGs by RT-qPCR analysis and western blotting. Among these hub genes, PSAT1 was considered to be an important regulator of the serine family amino acid biosynthetic process, which contributed to the invasion and migration of ESCC cells (19,20). VEGFA was associated with tumor angiogenesis (21). Hence, these two genes were selected for verification of DEGs. As shown in Fig. 4A-C, RT-qPCR and western blot assays revealed that the ectopic expression of MEG3 significantly downregulated the mRNA and protein expression of PSAT1 and VEGFA in EC109 cells, which was consistent with the results of microarray analysis (FC >2.0 or <0.5; P<0.05; Table II).

MEG3 inhibits the PSAT1-dependent GSK-3β/Snail signaling pathway. Accumulating evidence has demonstrated that the phenotypic changes of increased motility and invasiveness of cancer cells are associated with EMT. The GSK-3β/Snail signaling pathway plays an important role in the EMT process. GSK-3β has been reported to regulate Snail activity, and Snail triggers the EMT process by repressing E-cadherin expression (22). Sun *et al* reported that PSAT1 may activate the GSK-3β/Snail signaling pathway (23). To further confirm
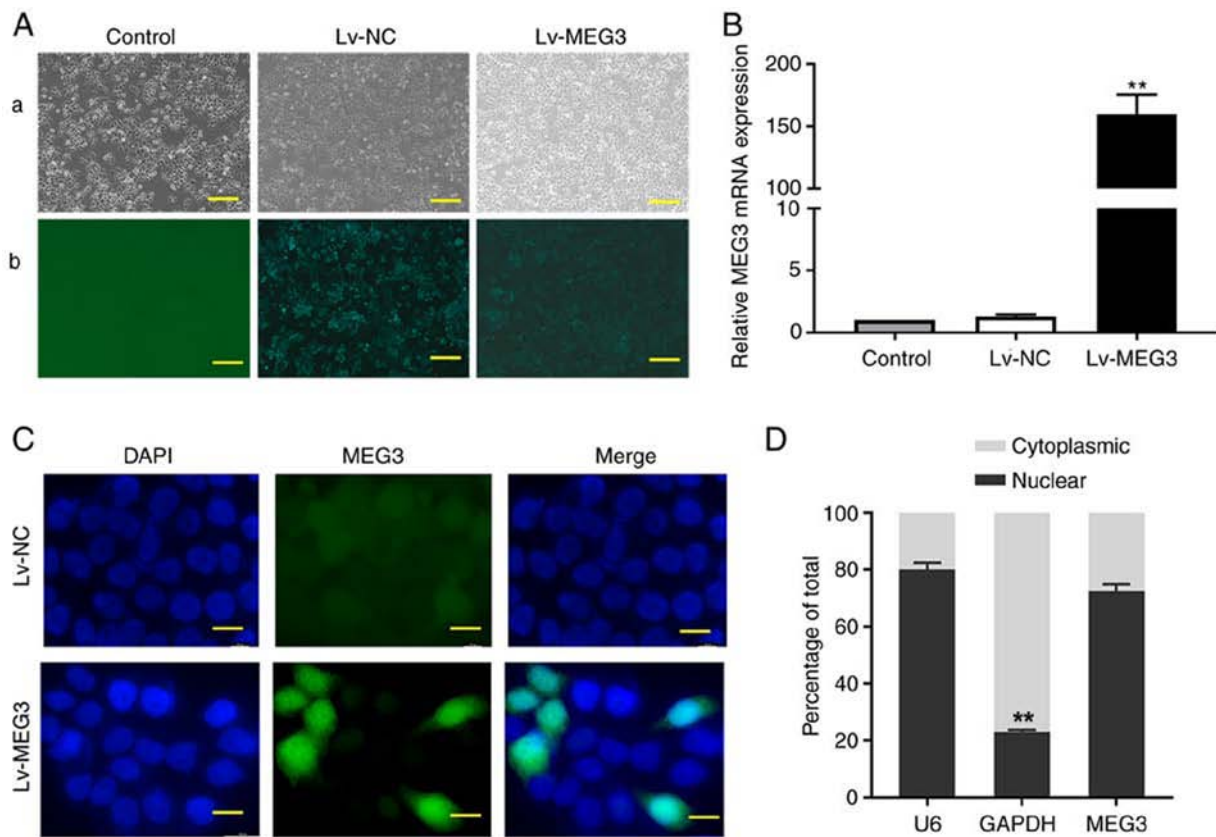
Figure 2. Ectopic expression of MEG3 and its subcellular location in EC109 cells. (A) Representative images of EC109 cells transfected with Lv-MEG3 or Lv-NC (magnification, x100; scale bar, 100 μm): (a) Bright image; (b) fluorescence image. (B) The ectopic expression of MEG3 in the Lv-MEG3 group was significantly higher compared with that in the control or Lv-NC groups by RT-qPCR assay. (C) Fluorescence *in situ* hybridization assay was performed to detect the distribution of MEG3 in EC109 cells (magnification, x1,000; scale bar, 10 μm). EC109 cells were co-stained with MEG3 anti-digoxin-HRP antibody (green) and DAPI (nucleus, blue). (D) Nuclear and cytoplasmic fractions of MEG3 in EC109 cells were evaluated by RT-qPCR with U6 or GAPDH as a nuclear or cytoplasmic internal control (**P<0.01). MEG3, maternally expressed gene 3; RT-qPCR, reverse transcription-quantitative PCR; NC, negative control; Lv, lentiviral vector.

the role of MEG3-mediated suppression of PSAT1 and its correlation with the GSK-3β/Snail signaling pathway, western blotting was performed. The results revealed that the ectopic expression of MEG3 significantly downregulated the level of the active form of GSK-3β (p-GSK-3β), but did not affect the total GSK-3β level (Fig. 4D and E). Overexpression of MEG3 also significantly downregulated the mean ratio of p-GSK-3β to total GSK-3β compared with the control group (Fig. 4F). In addition, ectopic expression of MEG3 in EC109 cells suppressed the molecular alterations that are character-istic of EMT (downregulation of the mesenchymal markers Snail and vimentin, and upregulation of the epithelial marker E-cadherin; Fig. 4D-H). Since the downregulation of PSAT1 is triggered by the overexpression of MEG3, it was inferred that MEG3 inhibits the PSAT1-dependent GSK-3β/Snail signaling pathway in EC109 cells.

Ectopic expression of MEG3 inhibits xenograft ESCC growth and PSAT1 expression in vivo. To demonstrate the effects of MEG3 on cancer cell dynamics *in vivo*, a xenograft tumor model in nude mice was constructed. MEG3-overexpressing (Lv-MEG3) and control cells (Lv-NC) were injected into the back flank of nude mice. The results demonstrated that ectopic expression of MEG3 significantly inhibited tumor growth (Fig. 5A-C). The maximum percentage weight loss

from start to end point in the experimental group was 10.51%, while in the control group it was 5.58%. Overexpression of MEG3 decreased PSAT1 expression and increased E-cadherin expression (Fig. 5D and E), indicating that MEG3 is involved in the regulation of EMT *in vivo*.

Expression of MEG3 and PSAT1 in clinical ESCC tissues and association with prognosis. To investigate the clinical relevance of MEG3 and PSAT1 in the progression of ESCC, and to further validate the microarray results, the present study focused on clinical relevance. After the mRNA levels of MEG3 were evaluated in 43 pairs of ESCC, the expression levels of PSAT1 were also examined by immunohistochemical staining. The results demonstrated that the expression levels of PSAT1 were markedly upregulated in ESCC tissues compared with those in adjacent normal tissues (Fig. 5G). Spearman's analysis revealed that the expressions of MEG3 and PSAT1 were negatively correlated in ESCC tissues (Pearson's r=-0.8314; P<0.0001; Fig. 5H). The survival analysis of patients using the Kaplan-Meier plotter website data (http://kmplot. com/analysis/) revealed that higher expression levels of PSAT1 tended to be correlated with a worse OS in Asian ESCC patients (hazard ratio=5.2; P=0.036; Fig. 5I). Taken together, these results indicate that MEG3 inhibits PSAT1 expression, and PSAT1 exerts a carcinogenic effect on ESCC.
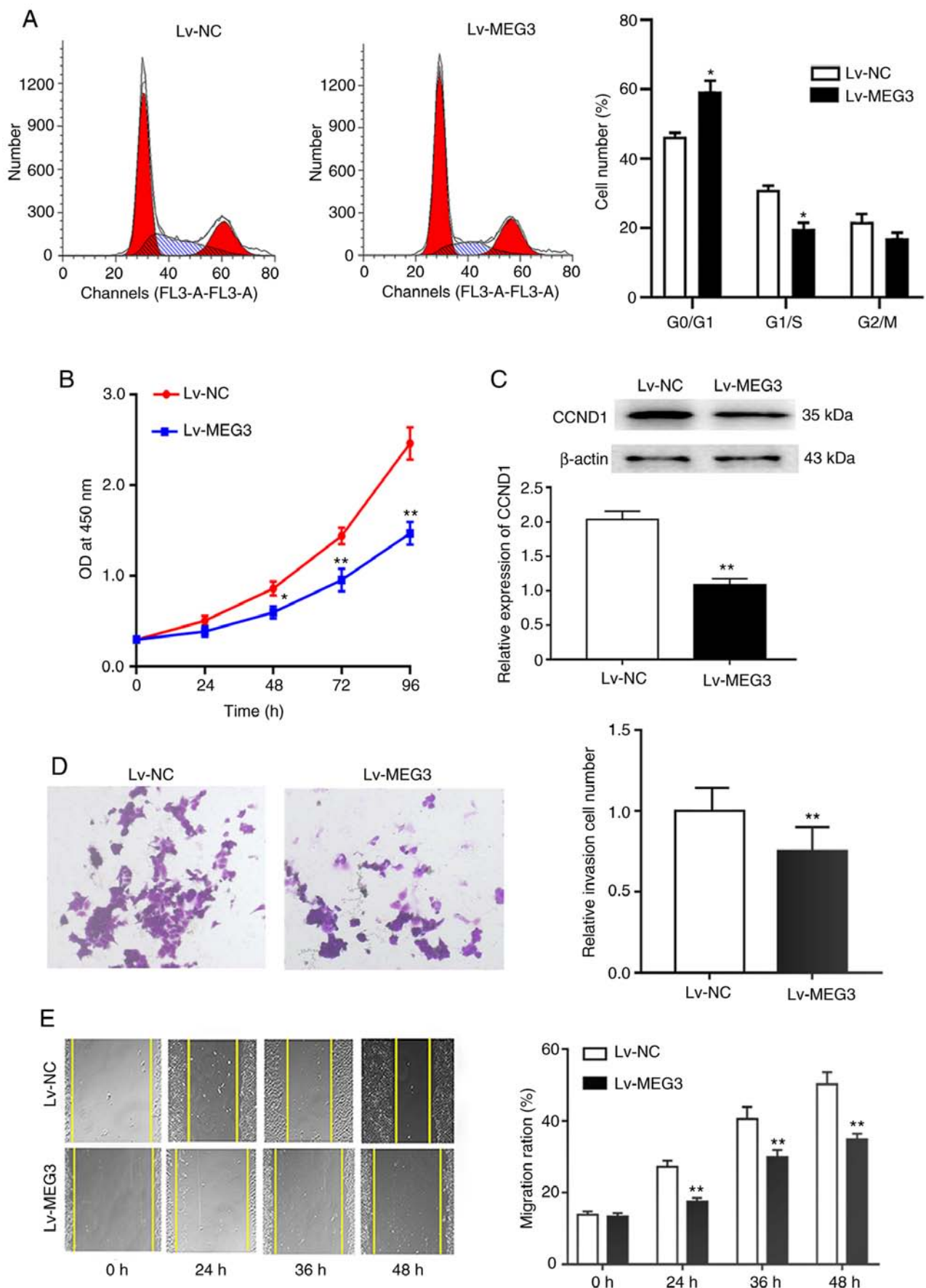
Figure 3. Ectopic expression of MEG3 suppresses the proliferation, migration and invasion of EC109 cells. (A) Flow cytometry assay indicated that overexpression of MEG3 resulted in G1/S cell cycle arrest. (B) Cell Counting Kit-8 assays indicated that ectopic expression of MEG3 suppressed the proliferation of EC109 cells. (C) Ectopic expression of MEG3 reduced the protein expression levels of CCND1. (D) Transwell assay demonstrated that MEG3 decreased the invasion of EC109 cells (magnification, x200). (E) Wound healing assay (magnification, x200). The wound width was measured with ImageJ software, and the results were plotted on the graphs (*P<0.05 and **P<0.01 in two-tailed Student's t-test). MEG3, maternally expressed gene 3; CCND1, cyclin D1.

Table II. All upregulated and top 30 downregulated genes in EC109 cells treated with Lv-NC and Lv-MEG3.

A, Upregulated genes

Gene symbol	Fold-change
CPA4	4.385887
PI3	3.580093
FABP5	3.568358
DKK1	3.321403
TFPI2	3.189393
IFIT1	3.157332
UBASH3B	2.757315
ABCG2	2.652196
C11orf86	2.631208
PRSS23	2.463662
EHF	2.462474
STXBP6	2.364241
NRXN3	2.362532
PLK2	2.298191
WDR4	2.250309
RPS26	2.215377
TNFRSF21	2.16497
HSPA8	2.148415
DDX6	2.095377
PGBD3	2.058019
DNAJA1	2.032604
AKR1C1	2.032215
FAM98A	2.01734

B, Downregulated genes

Gene symbol	Fold-change
INHBE	0.072167
ASNS	0.144524
NUPR1	0.14478
DDIT3	0.168082
ECM2	0.191233
PCK2	0.192793
CARS	0.198939
TRIB3	0.208346
SV2B	0.25678
CLGN	0.303193
AK7	0.320877
PHGDH	0.33101
GDPD1	0.331847
CEBPG	0.332314
PXK	0.348479
PRUNE2	0.36287
ARG2	0.368233
ATF4	0.372629
GARS	0.3881
PRG4	0.39037
MARS	0.393337
PSAT1	0.403129

Table II. Continued.

B, Downregulated genes

Gene symbol	Fold-change
GPT2	0.409617
AARS	0.410432
TUBE1	0.41201
DBNDD2	0.42243
SARS	0.42896
VEGFA	0.446095
TSPAN19	0.461047
TRIM2	0.461611

Fold-change >2.0 or <0.5; P<0.05. MEG3, maternally expressed gene 3; PSAT1, phosphoserine aminotransferase 1; VEGFA, vascular endothelial growth factor A.

Discussion

MEG3 has been proposed to play a biological role in various diseases, particularly cancer. Recent studies demonstrated that MEG3 is involved in the regulation of cancer-related pathways, and contributes to cell proliferation, metabolism, tumor progression and metastasis (9-14). In the present study, the expression and role of MEG3 in ESCC were assessed, and the mechanisms underlying its activity were investigated. The results demonstrated that MEG3 is downregulated in ESCC cell lines and tissues, and a lower level of MEG3 expression was associated with lymph node metastasis, TNM stage and poor prognosis in patients with ESCC. Ectopic expression of MEG3 inhibits cell viability and invasion *in vitro* and tumor formation by EC109 cells *in vivo*.

To explore the molecular mechanisms through which MEG3 regulates EMT in ESCC, the microarray results and KEGG pathway analysis were used, which demonstrated that biosynthesis of amino acids, aminoacyl-tRNA biosynthesis, serine and threonine metabolism, MAPK signaling pathway, alanine, and aspartate and glutamate metabolism were markedly enriched. Notably, another study also indicated that some aminoacyl-tRNA synthetases act as secreted cytokines to regulate angiogenesis and play a critical role in the tumor microenvironment (24). Emerging evidence indicates that serine and threonine metabolism, as well as alanine, aspartate and glutamate metabolism, are associated with tumor progression (25,26). The underlying mechanisms likely involve the regulation of the synthesis of proliferation-related proteins (27). Among those, one-carbon metabolism, a system of regulating cellular nutrient status, plays an important role in cancer (28,29). PSAT1, an enzyme that catalyzes the conversion of phosphoserine to serine, is highly expressed in various tumor tissues (19,30-34). Since PSAT1 was a hub gene in the PPI network and was identified as a DEG in the present study, the mechanism of MEG3 regulating EMT through PSAT1 was further investigated in EC109 cells.

E-cadherin mediates cell-cell adhesion, a characteristic that is lost during carcinogenesis. Decreased E-cadherin, and

Table III. Top 10 enrichment GO terms (BP, CC and MF) for the target genes of mRNAs.

GO ID	Term	Ontology	Count	Enrichment factor	P-value
GO:0009070	Serine family amino acid biosynthetic process	BP	4	29.73	1.47E-06
GO:0042149	Cellular response to glucose starvation	BP	4	16.4	1.84E-05
GO:0009069	Serine family amino acid metabolic process	BP	4	14.86	2.82E-05
GO:0006418	tRNA aminoacylation for protein translation	BP	5	12.39	1.23E-05
GO:0043039	tRNA aminoacylation	BP	5	11.66	1.7E-05
GO:0043620	Regulation of DNA-templated transcription in response to stress	BP	5	11.22	2.08E-05
GO:0086001	Cardiac muscle cell action potential	BP	4	11.06	0.000103
GO:0046626	Regulation of insulin receptor signaling pathway	BP	4	10.81	0.000113
GO:0043618	Regulation of transcription from RNA polymerase II promoter in response to stress	BP	4	10.12	0.000151
GO:0030968	Endoplasmic reticulum unfolded protein response	BP	9	9.31	2.42E-07
GO:0005829	Cytosol	CC	38	1.41	0.00357
GO:0015175	Neutral amino acid transmembrane transporter activity	MF	4	14.86	2.82E-05
GO:0030170	Pyridoxal phosphate binding	MF	4	9.15	0.000236
GO:0015179	L-amino acid transmembrane transporter activity	MF	4	8.97	0.000256
GO:0015171	Amino acid transmembrane transporter activity	MF	4	5.73	0.001781
GO:0008083	Growth factor activity	MF	5	3.69	0.005921
GO:0046943	Carboxylic acid transmembrane transporter activity	MF	4	3.63	0.0118
GO:0000982	RNA polymerase II core promoter proximal region sequence-specific DNA binding transcription factor activity	MF	9	3.3	0.001183
GO:0008236	Serine-type peptidase activity	MF	5	3.23	0.01106
GO:0017171	Serine hydrolase activity	MF	5	3.2	0.01163
GO:0001077	RNA polymerase II core promoter proximal region sequence-specific DNA binding transcription factor activity involved in positive regulation of transcription	MF	6	3.17	0.007246

GO, Gene Ontology; BP, biological process; CC, cellular component; MF, molecular function.

elevated Snail and vimentin expression are the most significant characteristics of EMT (35-38). Several signaling pathways, including MAPK/ERK, PI3K/AKT/GSK-3β and Wnt/β-catenin, are involved in EMT in ESCC (5,6,23,39,40). Liu *et al* reported that PSAT1 activates the GSK-3β/Snail signaling pathway and promotes the phosphorylation of GSK-3β. The latter further activates Snail and inhibits E-cadherin expression, leading to EMT in ESCC (20,31). In agreement with previous studies, the present study demonstrated that ectopic expression of MEG3 suppressed the migration and invasion of ESCC cells, and also decreased PSAT1 expression. Moreover, overexpression of MEG3 not only inhibited the phosphorylation of GSK-3β, Snail and vimentin expression, but also increased E-cadherin expression *in vitro*. In addition, the present study demonstrated that ectopic expression of MEG3 suppressed tumor growth, alongside PSAT1 downregulation and E-cadherin upregulation, indicating that MEG3 suppresses EMT by inhibiting the PSAT1-dependent GSK-3β/Snail signaling pathway in ESCC cells.

Based on the results of the *in vitro* studies, the expression and significance of PAST1 was examined in ESCC tissues

to confirm the findings in EC109 cell lines. The immunohistochemical results revealed that PSAT1 expression in tumor tissues was obviously higher compared with that in adjacent normal tissues, and MEG3 expression was significantly negatively correlated with PSAT1. The potential involvement of MEG3 and PSAT1 was confirmed by the Kaplan-Meier plotter website data in ESCC. Survival analysis of patients in the Asian population demonstrated that higher expression levels of PSAT1 were associated with poor prognosis. To the best of our knowledge, the present study was the first to demonstrate that MEG3 negatively regulates PSAT1 expression and the GSK-3β/Snail signaling pathway *in vitro* and *in vivo*, which may help improve our understanding of the anticancer mechanism of action of MEG3.

Notably, Dong *et al* reported that MEG3 inhibited EMT by competitively binding to miR-9 in YES2 cells (13). Xu *et al* demonstrated that the MEG3/miR-21 axis participates in the regulation of EMT in gastric cancer (41). In the present study, MEG3 inhibited EMT by inhibiting the PSAT1-dependent GSK-3β/Snail signaling pathway, suggesting that the mechanism of MEG3 regulating EMT varies across different cells,

Table IV. KEGG pathway enrichment analysis in DEGs.

Pathway name	P-value	Genes	FDR
Biosynthesis of amino acids	0.0010	CTH, ARG2, PHGDH, PSAT1, GPT2, CBS	1.24121
Biosynthesis of antibiotics	0.0016	CTH, ARG2, GFPT1, PHGDH, GGPS1, PSAT1, PCK2, AK7, CBS	1.96588
Aminoacyl-tRNA biosynthesis	0.0050	CARS, SARS, AARS, GARS, MARS	5.84549
Glycine, serine and threonine metabolism	0.0078	CTH, PHGDH, PSAT1, CBS	8.98694
MAPK signaling pathway	0.0518	ATF4, FGF12, CACNA1D, GADD45A, MAP2K6, DDIT3, HSPA8	46.9549
Alanine, aspartate and glutamate metabolism	0.0523	GFPT1, ASNS, GPT2	47.3064

KEGG, Kyoto Encyclopedia of Genes and Genomes; DEGs, differentially expressed genes; FDR, false discovery rate; MAPK, mitogen-activated protein kinase; PSAT1, phosphoserine aminotransferase 1.
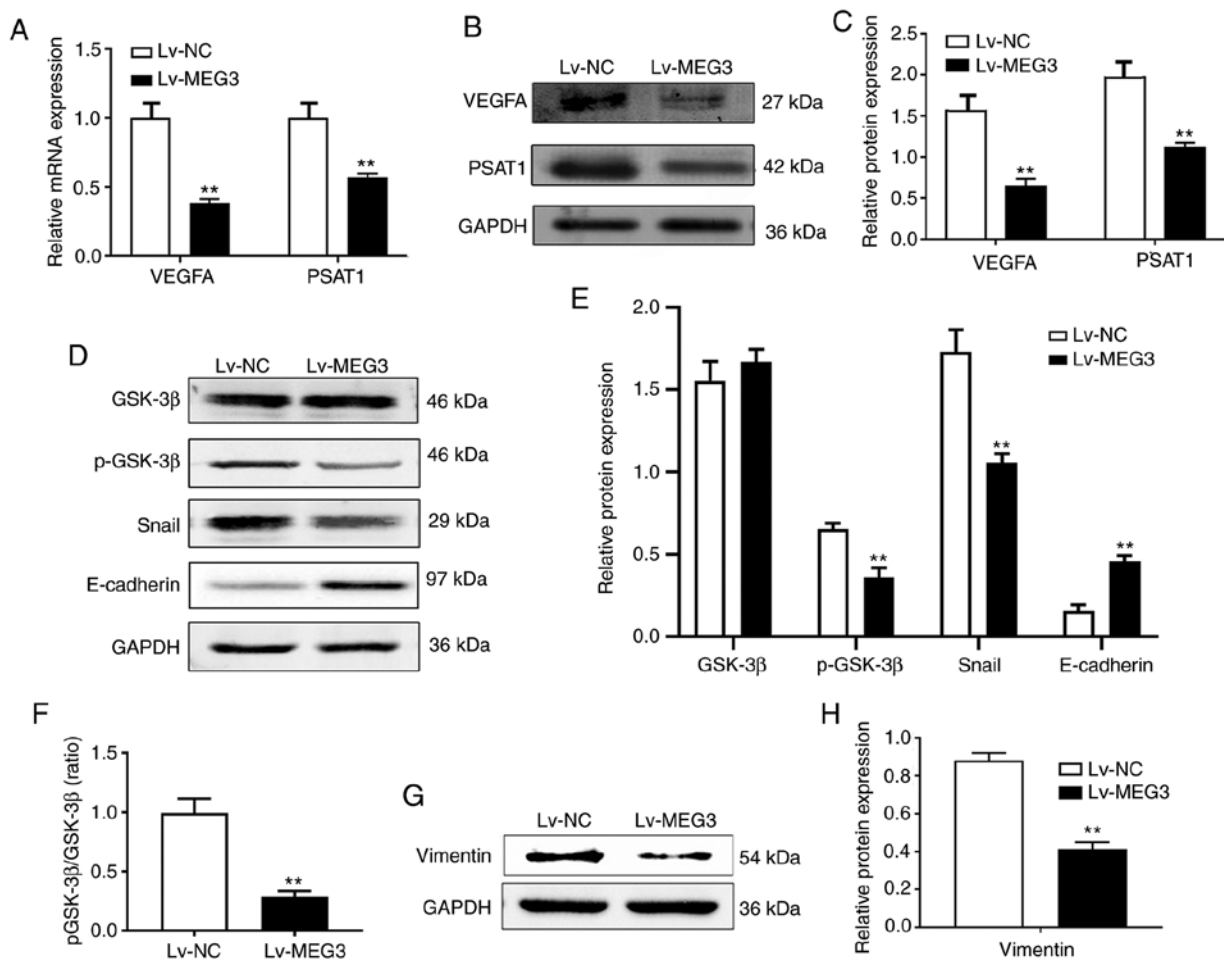

Figure 4. Validation of differentially expressed genes by reverse transcription-quantitative PCR, and effects of ectopic MEG3 on PSAT1-related signaling pathways in EC109 cells. (A) Decreased mRNA expression of PSAT1 and VEGFA was verified in EC109 cells transfected with Lv-MEG3. (B and C) Decreased protein expression of PSAT1 and VEGFA was verified in EC109 cells transfected with Lv-MEG3. (D and E) The relative protein levels of members of the GSK-3β/Snail signaling pathway were detected by western blot analysis. Ectopic MEG3 decreased the expression of phosphorylated GSK-3β and Snail, but increased the expression of E-cadherin. (F) The p-GSK-3β/GSK-3β ratio was compared between the Lv-NC and Lv-MEG3 groups. Ectopic expression of MEG3 decreased the p-GSK-3β/GSK-3β ratio. (G and H) Decreased protein expression of vimentin was observed in EC109 cells transfected with Lv-MEG3. The bars of the histograms indicate the mean ± SD of 3 independent experiments. $^{**}P<0.01$ compared with the Lv-NC group. MEG3, maternally expressed gene 3; Lv, lentiviral vector; NC, negative control; PSAT1, phosphoserine aminotransferase 1; VEGFA, vascular endothelial growth factor A; GSK, glycogen synthase kinase.

and there may be multiple mechanisms involved in the same cell type (7,36-38). The precise mechanism through which

MEG3 downregulates PSAT1 and EMT requires further investigation. In addition, only a limited number of samples
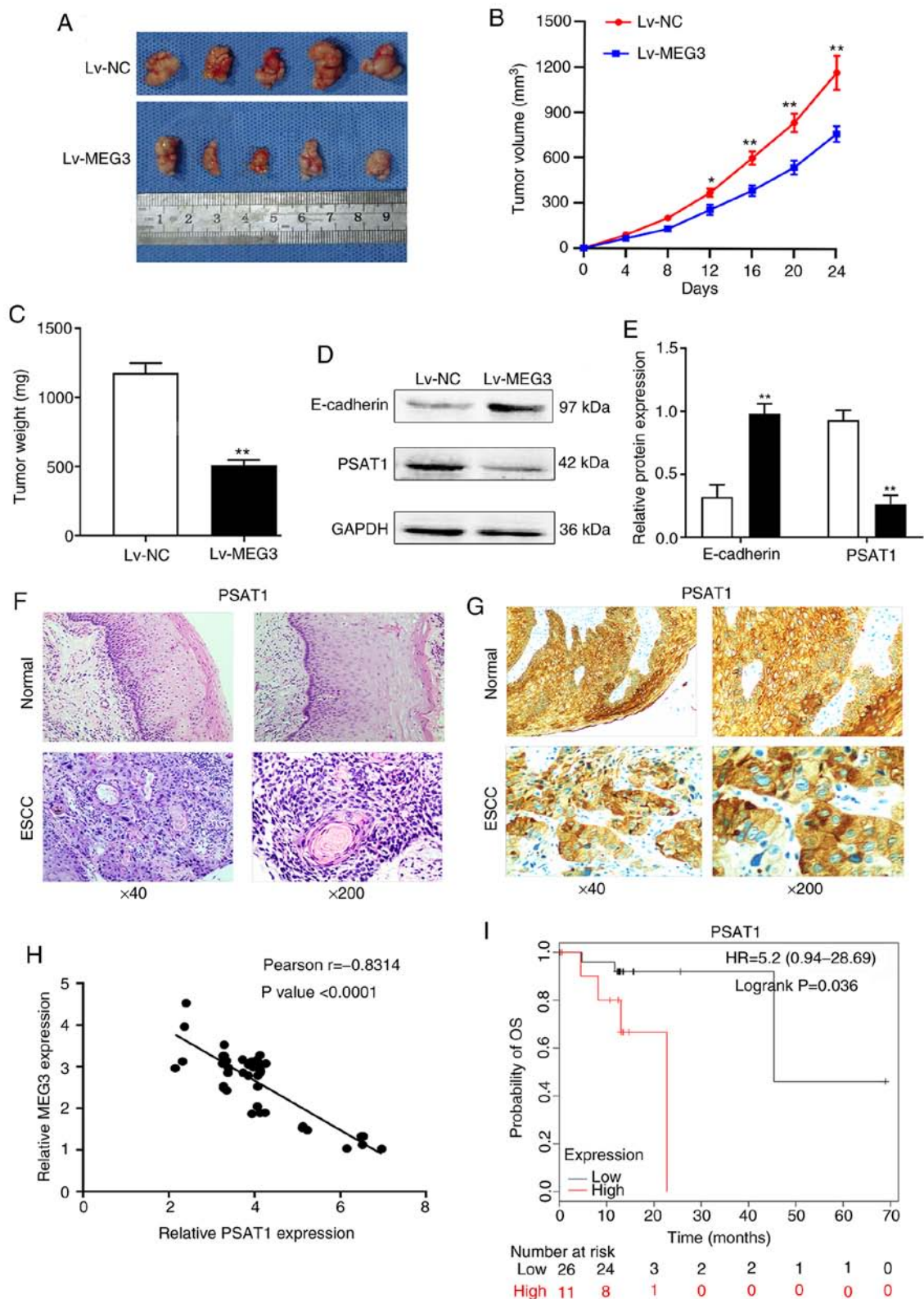
Figure 5. Ectopic expression of MEG3 disrupted tumor growth and PSAT1 expression *in vivo*, as was also shown by the association assay between MEG3 and PSAT1 in human ESCC. (A) *In vivo* resected tumors. Tumor (B) volume and (C) weight were significantly lower for cells with ectopic expression of MEG3 compared with Lv-NC cells. Mice were injected with Lv-MEG3 or Lv-NC cells and housed for 24 days. Tumor size was measured at weekly intervals. The results represent the mean ± SD of 5 mice in each group. (D and E) The protein levels of PSAT1 and E-cadherin were detected by western blotting in the tumor tissues. Ectopic MEG3 increased E-cadherin expression, but decreased PSAT1 expression. (F) Hematoxylin and eosin staining was performed on serial sections of ESCC and adjacent normal tissues. (G) Representative immunohistochemical staining for PSAT1 in ESCC samples and adjacent normal esophageal tissues. Positive staining (brown) was detected in tumor cells, but not in adjacent normal esophageal tissues. Original magnification x40, full, left; magnification x100, partial enlargement, right. (H) Relative expression of MEG3 and PSAT1 in 43 ESCC tissues, as determined by reverse transcription-quantitative PCR assay. The correlation between MEG3 and PSAT1 mRNA levels was determined by Pearson's correlation coefficient analysis. (I) Kaplan-Meier survival curves of patients with ESCC. The overall survival rates in patients with ESCC exhibiting low (n=59) or high (n=20) PSAT1 protein levels were significantly different (P=0.036). *P<0.05 and **P<0.01 compared with the Lv-NC group. MEG3, maternally expressed gene 3; Lv, lentiviral vector; NC, negative control; ESCC, esophageal squamous cell carcinoma; PSAT1, phosphoserine aminotransferase 1.

were examined in the present study. Future studies will include larger sample sizes to validate the correlation analysis.

In conclusion, the findings of the present study validated that MEG3 expression was decreased in human ESCC tissues, and was associated with tumor TNM stage and poor prognosis. The microarray results revealed that ectopic expression of MEG3 led to changes in major biological functions, including compound metabolic process and transcription. Furthermore, MEG3 appears to exert its effects through inhibiting the PSAT1-dependent GSK-3β/Snail signaling pathway in ESCC cells.

Availability of data and materials

The datasets used and/or analyzed during the present study are available from the corresponding author on reasonable request.

Authors' contributions

MKL performed the experimental work and contributed to figure preparation and writing of the manuscript. LXL contributed to gene microarray analysis and participated in the experiments. WYZ, HLZ and RPC assisted with the animal and molecular biology experiments. JLF contributed to data analysis. LFW designed and supervised the experiments. All the authors have read and approved the final manuscript.

Ethics approval and consent to participate

The clinical experiments were approved by the Ethics Committee of the Second Affiliated Hospital of Shantou University Medical College. Written informed consent was obtained from all the participants.

Patient consent for publication

Not applicable.

Competing interests

All the authors declare that they have no competing interests.

References

1. Bray F, Ferlay J, Soerjomataram I, Siegel RL, Torre LA and Jemal A: Global cancer statistics 2018: GLOBOCAN estimates of incidence and mortality worldwide for 36 cancers in 185 countries. CA Cancer J Clin 68: 394-424, 2018.

2. Wang SM, Abnet CC and Qiao YL: What have we learned from Linxian esophageal cancer etiological studies? Thorac Cancer 10: 1036-1042, 2019.

3. Xing L, Liang Y, Zhang J, Wu P, Xu D, Liu F, Yu X, Jiang Z, Song X, Zang Q and Wang W: Definitive chemoradiotherapy with capecitabine and cisplatin for elder patients with locally advanced squamous cell esophageal cancer. J Cancer Res Clin Oncol 140: 867-872, 2014.

4. Liu C, Tian X, Sun HB, Wang ZF, Jiang LF and Li ZX: MiR-601 inhibits the proliferation and metastasis of esophageal squamous cell carcinoma (ESCC) by targeting HDAC6. Eur Rev Med Pharmacol Sci 23: 1069-1076, 2019.

5. Hu X, Zhai Y, Kong P, Cui H, Yan T, Yang J, Qian Y, Ma Y, Wang F, Li H, et al: FAT1 prevents epithelial mesenchymal transition (EMT) via MAPK/ERK signaling pathway in esophageal squamous cell cancer. Cancer Lett 397: 83-93, 2017.

6. Yang JH, Wylie-Sears J and Bischoff J: Opposing actions of Notch1 and VEGF in post-natal cardiac valve endothelial cells. Biochem Biophys Res Commun 374: 512-516, 2008.

7. Thiery JP, Acloque H, Huang RYJ and Nieto MA: Epithelial-mesenchymal transitions in development and disease. Cell 139: 871-890, 2009.

8. Zhang H, Liu L, Wang Y, Zhao G, Xie R, Liu C, Xiao X, Wu K, Nie Y, Zhang H and Fan D: KLF8 involves in TGF-beta-induced EMT and promotes invasion and migration in gastric cancer cells. J Cancer Res Clin Oncol 139: 1033-1042, 2013.

9. Zhou Y, Zhang X and Klibanski A: MEG3 noncoding RNA: A tumor suppressor. J Mol Endocrinol 48: R45-R53, 2012.

10. Liu LX, Deng W, Zhou XT, Chen RP, Xiang MQ, Guo YT, Pu ZJ, Li R, Wang GF and Wu LF: The mechanism of adenosine-mediated activation of lncRNA MEG3 and its antitumor effects in human hepatoma cells. Int J Oncol 48: 421-429, 2016.

11. Zhang Z, Liu T, Wang K, Qu X, Pang Z, Liu S, Liu Q and Du J: Down-regulation of long non-coding RNA MEG3 indicates an unfavorable prognosis in non-small cell lung cancer: Evidence from the GEO database. Gene 630: 49-58, 2017.

12. Tan J, Xiang L and Xu G: LncRNA MEG3 suppresses migration and promotes apoptosis by sponging miR-548d-3p to modulate JAK-STAT pathway in oral squamous cell carcinoma. IUBMB Life 71: 882-890, 2019.

13. Dong Z, Zhang A, Liu S, Lu F, Guo Y, Zhang G, Xu F, Shi Y, Shen S, Liang J and Guo W: Aberrant methylation-mediated silencing of lncRNA MEG3 functions as a ceRNA in esophageal cancer. Mol Cancer Res 15: 800-810, 2017.

14. Pu Z, Wu L, Guo Y, Li G, Xiang M, Liu L, Zhan H, Zhou X and Tan H: LncRNA MEG3 contributes to adenosine-induced cytotoxicity in hepatoma HepG2 cells by downregulated ILF3 and autophagy inhibition via regulation PI3K-AKT-mTOR and beclin-1 signaling pathway. J Cell Biochem 120: 18172-18185, 2019.

15. Tai LW, Pan Z, Sun L, Li H, Gu P, Wong SSC, Chung SK and Cheung CW: Suppression of Pax2 attenuates allodynia and hyperalgesia through ET-1-ETAR-NFAT5 signaling in a rat model of neuropathic pain. Neuroscience 384: 139-151, 2018.

16. Zhou XT, Pu ZJ, Liu LX, Li GP, Feng JL, Zhu HC and Wu LF: Inhibition of autophagy enhances adenosine-induced apoptosis in human hepatoblastoma HepG2 cells. Oncol Rep 41: 829-838, 2019.

17. Huang ZL, Chen RP, Zhou XT, Zhan HL, Hu MM, Liu B, Wu GD and Wu LF: Long non-coding RNA MEG3 induces cell apoptosis in esophageal cancer through endoplasmic reticulum stress. Oncol Rep 37: 3093-3099, 2017.

18. Szklarczyk D, Franceschini A, Wyder S, Forslund K, Heller D, Huerta-Cepas J, Simonovic M, Roth A, Santos A, Tsafou KP, et al: STRING v10: Protein-protein interaction networks, integrated over the tree of life. Nucleic Acids Res 43 (Database Issue): D447-D452, 2015.

19. Yan S, Jiang H, Fang S, Yin F, Wang Z, Jia Y, Sun X, Wu S, Jiang T and Mao A: MicroRNA-340 inhibits esophageal cancer cell growth and invasion by targeting phosphoserine aminotransferase 1. Cell Physiol Biochem 37: 375-386, 2015.

20. Liu B, Jia Y, Cao Y, Wu S, Jiang H, Sun X, Ma J, Yin X, Mao A and Shang M: Overexpression of phosphoserine aminotransferase 1 (PSAT1) predicts poor prognosis and associates with tumor progression in human esophageal squamous cell carcinoma. Cell Physiol Biochem 39: 395-406, 2016.

21. Sabbah M, Emami S, Redeuilh G, Julien S, Prévost G, Zimber A, Ouelaa R, Bracke M, De Wever O and Gespach C: Molecular signature and therapeutic perspective of the epithelial-to-mesenchymal transitions in epithelial cancers. Drug Resist Updat 11: 123-151, 2008.

22. Xu W, Yang Z and Lu N: A new role for the PI3K/Akt signaling pathway in the epithelial-mesenchymal transition. Cell Adh Migr 9: 317-324, 2015.
23. Sun C, Zhang X, Chen Y, Jia Q, Yang J and Shu Y: MicroRNA-365 suppresses cell growth and invasion in esophageal squamous cell carcinoma by modulating phosphoserine aminotransferase 1. Cancer Manag Res 10: 4581-4590, 2018.
24. Kim S, You S and Hwang D: Aminoacyl-tRNA synthetases and tumorigenesis: More than housekeeping. Nat Rev Cancer 11: 708-718, 2011.
25. Man S, Li J, Fan W, Chai H, Liu Z and Gao W: Inhibition of pulmonary adenoma in diethylnitrosamine-induced rats by Rhizoma paridis saponins. J Steroid Biochem Mol Biol 154: 62-67, 2015.
26. Lane AN, Tan J, Wang Y, Yan J, Higashi RM and Fan TWM: Probing the metabolic phenotype of breast cancer cells by multiple tracer stable isotope resolved metabolomics. Metab Eng 43: 125-136, 2017.
27. Amelio I, Cutruzzolá F, Antonov A, Agostini M and Melino G: Serine and glycine metabolism in cancer. Trends Biochem Sci 39: 191-198, 2014.
28. Antonov A, Agostini M, Morello M, Minieri M, Melino G and Amelio I: Bioinformatics analysis of the serine and glycine pathway in cancer cells. Oncotarget 5: 11004-11013, 2014.
29. Possemato R, Marks KM, Shaul YD, Pacold ME, Kim D, Birsoy K, Sethumadhavan S, Woo HK, Jang HG, Jha AK, et al: Functional genomics reveal that the serine synthesis pathway is essential in breast cancer. Nature 476: 346-350, 2011.
30. The UniProt Consortium: UniProt: The universal protein knowledgebase. Nucleic Acids Res 45: D158-D169, 2017.
31. Dai J, Wei R, Zhang P and Kong B: Overexpression of microRNA-195-5p reduces cisplatin resistance and angiogenesis in ovarian cancer by inhibiting the PSAT1-dependent GSK3β/β-catenin signaling pathway. J Transl Med 17: 190, 2019.
32. Basurko MJ, Marche M, Darriet M and Cassaigne A: Phosphoserine aminotransferase, the second step-catalyzing enzyme for serine biosynthesis. IUBMB Life 48: 525-529, 1999.
33. Baek JY, Jun DY, Taub D and Kim YH: Characterization of human phosphoserine aminotransferase involved in the phosphorylated pathway of L-serine biosynthesis. Biochem J 373: 191-200, 2003.

34. Vié N, Copois V, Bascoul-Mollevi C, Denis V, Bec N, Robert B, Fraslon C, Conseiller E, Molina F, Larroque C, et al: Overexpression of phosphoserine aminotransferase PSAT1 stimulates cell growth and increases chemoresistance of colon cancer cells. Mol Cancer 7: 14, 2008.
35. Mishra R: Glycogen synthase kinase 3 beta: Can it be a target for oral cancer. Mol Cancer 9: 144, 2010.
36. Singh A and Settleman J: EMT, cancer stem cells and drug resistance: An emerging axis of evil in the war on cancer. Oncogene 29: 4741-4751, 2010.
37. Kiweler N, Brill B, Wirth M, Breuksch I, Laguna T, Dietrich C, Strand S, Schneider G, Groner B, Butter F, et al: The histone deacetylases HDAC1 and HDAC2 are required for the growth and survival of renal carcinoma cells. Arch Toxicol 92: 2227-2243, 2018.
38. Kiweler N, Wünsch D, Wirth M, Mahendrarajah N, Schneider G, Stauber RH, Brenner W, Butter F and Krämer OH: Histone deacetylase inhibitors dysregulate DNA repair proteins and antagonize metastasis-associated processes. J Cancer Res Clin Oncol 146: 343-356, 2020.
39. Jin Y, Xu K, Chen Q, Wang B, Pan J, Huang S, Wei Y and Ma H: Simvastatin inhibits the development of radioresistant esophageal cancer cells by increasing the radiosensitivity and reversing EMT process via the PTEN-PI3K/AKT pathway. Exp Cell Res 362: 362-369, 2018.
40. Coussens LM, Fingleton B and Matrisian LM: Matrix metalloproteinase inhibitors and cancer: Trials and tribulations. Science 295: 2387-2392, 2002.
41. Xu G, Meng L, Yuan D, Li K, Zhang Y, Dang C and Zhu K: MEG3/miR-21 axis affects cell mobility by suppressing epithelial-mesenchymal transition in gastric cancer. Oncol Rep 40: 39-48, 2018.